American Mineralogist, Volume 64, pages 1199–1218, 1979

The tetravalent manganese oxides: identification, hydration, and structural relationships by infrared spectroscopy

RUSSELL M. POTTER[1] AND GEORGE R. ROSSMAN

Division of Geological and Planetary Sciences[2]
California Institute of Technology
Pasadena, California 91125

Abstract

A compilation of the infrared powder absorption spectra of most naturally occurring tetravalent and trivalent manganese oxides is presented which is intended to serve as a basis for the spectroscopic identification of these minerals in both ordered and disordered varieties, including those too disordered for X-ray diffraction studies. A variety of synthetic manganese oxides are also included for comparison to the natural phases. The samples include: aurorite, birnessite, braunite, buserite, chalcophanite, coronadite, cryptomelane, groutite, hausmannite, hollandite, lithiophorite, manganite, manganese(III) manganate(IV), manganosite, manjiroite, marokite, nsutite, partridgeite, pyrolusite, quenselite, rancieite, ramsdellite, romanechite, sodium manganese(II,III) manganate(IV), todorokite, and woodruffite. The spectra indicate that well-ordered water occurs in ramsdellite, chalcophanite, and most romanechites. Disordered water is observed in the spectra of nsutite, hollandites, birnessite, todorokite, buserite, and rancieite. The infrared spectra of well-ordered todorokite, birnessite and rancieite differ which indicates that they possess different structures and should be regarded as distinct mineral species. Much variation is observed in the spectra of pyrolusites, nsutites, birnessites, and todorokites which is interpreted as arising from structural disorder. Spectral trends suggest that todorokite, birnessite and rancieite have layered structures.

Introduction

The finely-particulate and disordered nature of manganese oxides in many of their concentrations in the weathering environment has made identification of their mineralogy by means of X-ray diffraction difficult and sometimes impossible. Characteristic X-ray powder diffraction lines are frequently broad, indistinct, or absent altogether and do not serve as a satisfactory basis for identification. The frequent occurrence of silicate phases admixed with the low-temperature manganese oxides is an additional complication because their X-ray lines can sometimes be confused with those of the manganese oxides.

Problems of particle size and disorder are a characteristic of pure manganese oxides and have been responsible for our poor understanding of manganese oxide crystal structures and structural relationships. X-ray powder diffraction patterns are the only structural data available on several of the oxides important in the weathering environment, and these generally show lines which are few in number, broad, and sometimes variable in position. This has caused uncertainty in the structural relationships among synthetic and natural samples and a consequent confusion in their classification.

This work will show that infrared (IR) spectroscopy is often a necessary alternative and generally a useful supplement to X-ray diffraction for mineralogical analysis of the manganese oxides. Because it is sensitive to amorphous components and those with short-range order as well as to material with long-range order, IR spectroscopy yields a more complete and reliable description of materials such as the manganese oxides, where crystalline disorder may be expected. In addition, it is sensitive to the structural environment of the hydrous components, which is

[1] Present address: Owens-Corning Fiberglas Corporation, Granville, Ohio 43023.

[2] Contribution No. 3126.

0003–004X/79/1112–1199$02.00

frequently diagnostic of the manganese oxide mineralogy.

Because IR spectroscopy is not a primary structural technique like X-ray diffraction, it is necessary to "calibrate" it against well-crystallized materials whose mineralogy has been previously determined by X-ray diffraction. Once a mineral's characteristic IR spectrum has been determined, it can then be used to identify whether that phase is present in more disordered samples.

More than 20 predominantly tetravalent manganese oxide phases are recognized as valid mineral species. X-ray criteria for the identification of the well-crystallized oxides are well established (Cole *et al.,* 1947; Burns and Burns, 1977a). This paper presents the basis for determination of their mineralogy by IR spectroscopy. The IR spectra of many of the manganese oxides have been published (Gattow and Glemser, 1961a, b; Glemser *et al.,* 1961; Moenke, 1962; Valarelli *et al.,* 1968; Agiorgitis, 1969; Kolta *et al.,* 1971; van der Marel and Beutelspacher, 1976), but the quality of the data are generally too poor to show clear differences among the oxides. Using improved instrumentation and sample preparation techniques, we have found that the differences in the IR spectra of the tetravalent manganese oxides are sufficiently diagnostic to permit their identification in manganese oxide concentrations of the natural environment even when the oxides are highly disordered. We have used these spectra as the basis for the determination of manganese mineralogy in a variety of occurrences including desert varnish, manganese dendrites, stream deposits, and concretions (Potter and Rossman, 1979a, b, c).

This paper also contains the results of research into some fundamental problems of tetravalent manganese oxide mineralogy. We have used our spectroscopic results in conjunction with a variety of other techniques to investigate structural variations within the manganese oxides, to address questions about the doubtful structures, to propose structural models for structures which are as yet unknown, and to test the validity of synthetic materials as analogs of natural samples.

The presentation of these results follows the classification scheme of Burns and Burns (1975, 1977a, b), which is based on the nature of the polymerization of MnO_6 units, in which six oxygens surround a central manganese cation in approximately octahedral coordination. For each structure representative spectra are included with the text. Spectra of other samples are contained in Appendix B as indicated in Table 1. Appendix figures are indicated by an "A" or "B" following the figure number.[3] The intensities of IR spectra may vary by a factor of 2 or 3 due to differences in sample particle size and dispersion in the pellet. For this reason we have presented the IR spectra at concentrations such that all spectra have the same maximum intensity in the 1400 cm^{-1} to 200 cm^{-1} region. Each spectrum in the 4000 cm^{-1} to 1400 cm^{-1} region is presented at 4 times the concentration of its lower energy spectrum. The presentation intensities listed in the figure captions allow the original intensity of the spectra to be calculated. The presentation intensity is 100 times the intensity in the figure divided by the intensity measured using the standard preparation techniques (Section 2).

Experimental details

Purity and mineralogy were determined by X-ray powder diffraction using Cr$K\alpha$ radiation and a Debye-Scherrer camera. The IR spectrum of some minerals is so distinctive that after an initial correlation was made between the X-ray diffraction pattern and the IR spectrum, further X-ray work was not needed. When necessary, qualitative chemical analysis was used in addition to X-ray diffraction to determine mineralogy.

IR spectra were obtained with a Perkin-Elmer model 180 spectrophotometer on 2.0 mg of powdered sample dispersed in TlBr pellets for the 4000 cm^{-1} to 1400 cm^{-1} region and on 0.5 mg in TlBr and KBr pellets for the 1400 cm^{-1} to 200 cm^{-1} region. Pellets of 13 mm diameter were pressed for 1 minute at 19,000 psi under vacuum. Pellets were prepared without evacuation to verify that dehydration of the manganese oxide did not occur under these conditions. Since KBr is hygroscopic, it was not used in the 4000 cm^{-1} to 1400 cm^{-1} region, where water and hydroxide absorption occurs. TlBr is preferable to KBr because it is non-hygroscopic. Also, because its refractive index better matches most manganese oxides, it gives spectra of better quality. The figures presented are from TlBr pellets. Where the corresponding spectrum in KBr differs significantly, it is included in Appendix B. A vacuum dewar with KBr windows was used to obtain IR spectra at liquid nitrogen temperature in the 4000 cm^{-1} to 1400 cm^{-1} region. Qualitative chemical analyses were done with an SEM

[3] To receive a copy of Appendices A and B and a table of IR band positions, order Document AM-79-117 from the Business Office, Mineralogical Society of America, 2000 Florida Avenue, NW, Washington, D. C. 20009. Please remit $1.00 in advance for the microfiche.

equipped for energy dispersive X-ray analysis. Manganese oxidation state was determined by room temperature dissolution in excess 0.05M Fe^{2+} in 0.5M H_2SO_4 followed by back titration of excess Fe^{2+} with 0.002M $KMnO_4$ and spectrophotometric determination of total Mn as MnO_4^-. This procedure is a modification of that of Moore *et al.* (1950). Far-infrared spectra in the region 200 cm^{-1} to 35 cm^{-1} were obtained from a petroleum jelly mull of 10 mg of sample spread on a polyethylene plate.

The chain structures: pyrolusite, nsutite, ramsdellite

Pyrolusite

Two structural forms of pyrolusite are thought to exist (de Wolff, 1959): a tetragonal form, which is characteristic of pyrolusite of primary origin, and an orthorhombic modification characteristic of pyrolusite formed by alteration of manganite. A single-crystal X-ray structural determination has not been done for pyrolusite. The tetragonal structure (Fig. 1) is based on X-ray powder diffraction data. MnO_6 octahedra share edges to form single chains linked to one another by shared vertices along the *c* axis. De Wolff postulated the existence of an orthorhombic modification from broadening of several X-ray powder lines. Electron microscopy has revealed oriented lamellar pores in secondary pyrolusites which could be responsible for this distortion (Champness, 1971).

The X-ray powder patterns of Figure 2 confirm the existence of an orthorhombic pyrolusite. The pyrolusite patterns are arranged in order of increasing broadness of the following lines (indices in parenthesis): 2.20A (200), 1.97 (210), 1.62 (211), 1.391 (310), 1.305 (301), 1.20 (202). The (301) line is superimposed on that of (112), which does not split. For pyrolusite #4 several of these lines are clearly-resolved doublets, and the overall pattern can be indexed to an orthorhombic cell bearing the following relation to the undistorted pyrolusite cell:

tetragonal	orthorhombic
$a = 4.42$A	$c = 4.44$A
	$a = 4.36$A
$c = 2.87$A	$b = 2.87$A

The IR spectra of this pyrolusite series show considerable variation. The order of the spectra in Figure 3 is the same as that of the powder patterns in Figure 2. The spectral variations are not well correlated with X-ray patterns, although two trends are suggested in going from top to bottom in Figure 3; the resolution of bands 3,4, and 5 improves, and the intensity of band 3 grows with respect to band 4.

All the pyrolusite powder diffraction patterns contain lines at 3.40, 2.63, 2.32, 1.78, and 1.71A. These cannot be indexed on the tetragonal pyrolusite cell nor on a superlattice of it. They can all be attributed to manganite and account for its four strongest lines. The +3.99 manganese oxidation state of pyrolusite #11 limits its possible manganite contamination to 1 percent. Although other pyrolusite samples could have up to 8 percent manganite, their unindexed X-ray lines are not measurably stronger than those of pyrolusite #1. IR spectroscopy limits the amount of manganite impurity to less than 5 percent for all samples, based on the intensity of the band near 1100 cm^{-1}. This feature may alternatively be attributed to some other hydroxide ion impurity or to an overtone of the intense absorption at lower wavenumber. At present it seems likely that most pyrolusite samples contain a small amount of manganite impurity, but we do not feel that the evidence is conclusive.

The variation in the pyrolusite IR spectra of Figure 3 is representative for pyrolusite samples in general and is a problem in its own right. The primary difference among the spectra is the position and relative intensity of band 3. Farmer (1974) has considered the effect particle shape would theoretically have on the IR spectra of rutile, which is isostructural with pyrolusite and has a spectrum similar to it. He suggested that shape may be the cause of large variations in the IR spectra of different powdered rutile samples. The major variation in going from a platy to a needle-like morphology is predicted to be a decrease of several hundred wavenumbers in the position of band 3, which is similar to the variations we observe for pyrolusite. Although scanning electron microscopy did show variation in particle shape from needles to equant particles, this variation could be generated for a single sample by different grinding techniques with no effect on the position of band 3. It thus appears that particle shape is not responsible for the variation in pyrolusite IR spectra.

Polarized reflectance spectra of pyrolusite #5 indicate that bands 1, 2, and 4 are polarized perpendicular to the *c* axis and that band 3 is polarized parallel to the *c* axis. Band 5 is not present in the spectra of pyrolusite #5, which is our only sample with single crystals large enough to yield reflectance spectra. These results are in complete agreement with the predictions of factor group analysis for the tetragonal pyrolusite structure. Band 3 is due to the displacement of the oxygen ions relative to the manga-

Table 1. Sample information.

	sample #	locality	ident. #	ref. #	fig. #	purity x-ray	purity IR	chemistry
Pyrolusite	1	Germany	CIT 2853		1B	pure	pure	
MnO_2	2	Rossbach, Westphalia	CIT 4511		1B	pure	pure	
	3	Lake Valley, New Mexico	CIT 2402		1B	m,ram	pure	
	4	Nissan, Germany	HAV 93614		3,1B	pure	pure	58.3% Mn:(+3.96)
	5	Lake Valley, New Mexico	HAV 111929	2	2B	pure	pure	
	6	Sierra County, New Mexico	LCM 10995	2	3	pure	pure	59.5% Mn;(+3.94)
	7	Central New Mexico	CIT 2731		2B	pure	pure	
	8	Locality unknown	CIT 9430		2B	pure	pure	
	9	Synthetic	CIT 9431	3	3	pure	pure	60.0% Mn;(+3.92)
	10	Synthetic	CIT 9432	4	3	pure	pure	60.4% Mn;(+3.98)
	11	Synthetic	CIT 9433	5	3	pure	pure	61.8% Mn;(+3.99)
Nsutite	12	Nsută, Ghana	CIT 9434		3B		pure	
$Mn(O,OH)_2 \cdot xH_2O$	13	Salmchateau, Belgium	CIT 9196	6			m,cla	
	14	Hidalgo, Mexico	HWT M-23		4	pure	t,pyr	59.6% Mn;(+3.97)
	15	Oxen Claim, Utah	HWT UT-17	6			m,qtz	
	16	Synthetic	CIT 9435	7	5,3B	pure	pure	
	17	Synthetic	CIT 9436	8	4	pure	pure	58.4% Mn;(+3.63)
	18	Synthetic	CIT 9437	9	4,6,3B	pure	pure	59.5% Mn;(+3.89)
	19	Synthetic	CIT 9438	10	4	pure	pure	58.6% Mn;(+3.89)
Ramsdellite	20	Chihuahua, Mexico	CIT 9439	11	7	pure	pure	
MnO_2	21	Black Magic Mine, Calif.	CIT 9440		4B	t,hol	t,hol	
	22	Lake Valley, New Mexico	CIT 7486	12	4B	t,pyr	t,pyr	
Hollandite group	23	Broken Hill, N.S.W.	CIT 3523		5B		pure	*Mn,Pb,Si
Coronadite	24	Bou Tazoutt, Morocco	HWT MOR-6	13,14	5B		pure	*Mn,Pb,V
$PbMn_8O_{16}$	25	Inyo Co., Calif.	HAV 111927				M,qtz.	*Mn,Pb,Si
Cryptomelane	26	Chihuahua, Mexico	CIT 9441	13	6B	t,tod	pure	*Mn,K,Ni,Fe
KMn_8O_{16}	27	Patagonia Mine, Arizona	HWT AR-22	13	9	pure	pure	*Mn,K
	28	Tiouine, Morocco	HWT MOR-1			t,qtz, brn	t,qtz	*Mn,K,Ba,Si,Al
	29	White Oak Mtn., Tenn.	HWT E-23		6B		pure	*Mn,K,Al,Si,Ba
	30	Synthetic	CIT 9442	15	6B	pure	pure	*Mn,K
Hollandite	31	Soharis, Sweden	LCM 13875	14	7B		pure	*Mn,Ba,K,Ca,Fe,Al,Si
$BaMn_8O_{16}$	32	Synthetic	CIT 9443	15	7B		pure	*Mn,Ba
Manjiroite $NaMn_8O_{16}$	33	Synthetic	CIT 9444	15	7B		pure	
Romanechite	34	Chihuahua, Mexico	CIT 9445	16	8B	pure	pure	
(Psilomelane)	35	Palos Verdes Hills, Calif.	CIT 9446	17	8B		t,brn	
$(Ba,H_2O)_2Mn_5O_{10}$	36	Mayfield Prospect, Texas	HWT, T-2		8B		pure	
	37	Pribble Mine, Virginia	HWT, E-48		10B,8B		pure	
	38	Van Horne, Texas	HAV 97618	18	10	pure	pure	
Chalcophanite group								
Aurorite $(Mn,Ag,Ca)Mn_3O_7 \cdot 3H_2O$	39	Aurora Mine, Nevada	HST LU-21	19,20	9B		t,qtz	*Mn,Si,Ca,Cu,Ag,Zn,K,Ba
Chalcophanite	40	Sterling Hill, New Jersey	CIT 406	13,21	12,9B	pure	pure	
$ZnMn_3O_7 \cdot 3H_2O$	41	Sonora, Mexico	CIT 7134		9B		t,qtz	
Lithiophorite	42	Postmasburg, S. Africa	CIT 9447	22	13		pure	
$(Al,Li)MnO_2(OH)_2$	43	Sausalito, Calif.	CIT 7968		13,10B		pure	
	44	Greasy Cove, Alabama	HWT E-14	22	10B		pure	
Birnessite	45	Mt. St. Hilaire, Quebec	CIT 8509		11B	t,ser	m,ser	
$(Na,Ca,K)Mn_7O_{14} \cdot 3H_2O$	46	Boron, Calif.	CIT 9448	23		pure	t,sil	
	47	Cummington, Mass.	NMNH 115315	24	14	pure	t,cbn?	49.4% Mn;(+3.70)
	48	Synthetic, K	CIT 9449	25	11B	pure	pure	
	49	Synthetic, K	CIT 9450	26	14,11B	pure	pure	58.0% Mn;(+3.94);*Mn,K
	50	Synthetic, K	CIT 9451	27	14,11B	pure	pure	48.8% Mn;(+3.90)
	51	Synthetic, Mn	CIT 9452	28	14		pure	*Mn
	52	Synthetic, Na	CIT 9453	26	12B	pure	pure	*Mn,Na
	53	Synthetic, Ca	CIT 9454	26	12B	pure	pure	*Mn,Ca
	54	Synthetic, Na	CIT 9455	29	14	pure	pure	

nese ions along the direction of the octahedral chains (by analogy with isostructural rutile; Farmer, 1974). It is variation in the vibration frequency of this movement which is responsible for the major variation in the pyrolusite spectra, but it does not suggest any structural variation which may be its cause. The following section on nsutite will show that the presence of ramsdellite double chains is not responsible for the variation in the position of band 3, although it may be responsible for the presence of band 5 and

Table 1. (continued)

Todorokite group	55	Palos Verdes Hills, Calif.	CIT 9456	17	15,13B		t,sil?	
Todorokite	56	Chihuahua, Mexico	CIT 9457	11	13B		pure	
$(Mn,Ca,Mg)Mn_3O_7 \cdot H_2O$	57	Chihuahua, Mexico	CIT 9458	11	15		t,sil	
	58	Bombay, India	CIT 9459		15		pure	
	59	Miramati Mine, Japan	CIT 9460		13B		m,mgn	
	60	Charco Redondo, Cuba	CIT 9733	30	15		pure	
	61	Unknown locality	HWT Mn-24	30	15		pure	
Woodruffite	62	Sterling Hill, New Jersey	NMNH 114158	31	13B		pure	*Mn,Zn,Cu,Ca,Al
$(Zn,Mn)Mn_3O_7 \cdot H_2O$								
Rancieite	63	Paxton's Cave, Virginia	NMNH 120601	32	17	pure	pure	
$(Ca,Mn)Mn_4O_9 \cdot 3H_2O$	64	Rancié Mtns., France	NMNH 128319	21, 32	17	t,tod	t,sil	
	65	Orienta Province, Cuba	HAV 110334	32	17,14B	m,brn	m,brn	
	66	Itia, Greece	CIT 9430	33	14B		pure	
Buserite	67	Synthetic	CIT 9622	34	16	pure	pure	
$(Na,Mn)Mn_3O_7 \cdot xH_2O$	68	Synthetic, Co	CIT 9623	34	15B	pure	pure	
	69	Synthetic, Mn	CIT 9677	34	15B	m,bir, imp	pure	

1. The following abbreviations are used for sample identification numbers: CIT = California Institute of Technology, HAV = Harvard University, LCM = Los Angeles County Museum of Natural History, HWT = The Hewett Collection in possession of the U. S. Geological Survey at Denver, Colorado, NMNH = National Museum of Natural History, The Smithsonian Institution; for X-ray and IR purity M indicates major impurities, m indicates minor impurities, t indicates trace impurities. Samples are indicated to be X-ray pure despite the presence of several weak lines which do not match other standard samples provided that these cannot be attributed to other phases. This was generally the case for the hollandite group and birnessite. The special case of pyrolusite is discussed in the text. For X-ray and IR purity the following abbreviations are used: bir = birnessite, brn = braunite, cbn = carbonate, cla = clay minerals, hol = hollandite, imp = unidentified impurity, mgn = manganite, pyc = pyrochroite, pyr = pyrolusite, qtz = quartz, ser = serandite, sil = silicate, tod = todorokite. Under chemistry the manganese oxidation state is enclosed in parentheses. Following *, elements detected by qualitative analysis are listed in approximate order of concentration; elements in trace quantity are underlined. The chemical formulae included in this table should be taken as only an approximate indication of the chemistry of the mineral phases. The variations in cation substitution, manganese oxidation state, hydration, and structure preclude a single rigorous chemical formula for many of the minerals.
2. Mislabeled as ramsdellite in the collections.
3. Synthetic method: McKenzie, 1971.
4. Artificial δ-MnO_2; from National Carbon Company.
5. Manganese dioxide HP; from Diamond Shamrock Chemical Company, Baltimore, Maryland; 99.9% MnO_2, 0.005% Fe by their analysis.
6. Zwicker et al., 1962.
7. Synthetic method: preparation a for η" - MnO_2 from Gattow and Glemser, 1961a.
8. Synthetic method: electrolytic preparation for η - MnO_2 from Gattow and Glemser, 1961a.
9. Synthetic method: Giovanoli et al., 1967.
10. Synthetic method: Giovanoli et al., 1967, 10.0 N HNO_3 was used in place of 1.0 N HNO_3.
11. Finkelman et al., 1974.
12. Apparently a poor sample of Lake Valley ramsdellite since the ramsdellite structure was determined on material from Lake Valley.
13. Palanche et al., 1944.
14. Byström and Byström, 1950.
15. Synthetic method: preparation #1, McKenzie, 1971; $Ba(MnO_4)_2$ and $NaMnO_4$ were used in place of $KMnO_4$ for synthesis of hollandite and manjiroite respectively.
16. The locality is described in Finkelman et al., 1974.
17. The locality is described in Mitchel and Corey, 1973.
18. Fleischer, 1960
19. Radtke et al., 1967.
20. Prior to analysis major calcite impurity was removed by 10 minute treatment with dilute acetic acid followed by washing with deionized water.
21. Wadsley, 1955.
22. Fleischer and Faust, 1962.
23. Brown et al., 1971.
24. Frondel et al., 1960a.
25. Synthetic method: The first preparation for δ-MnO_2 from Glemser et al., 1961.
26. Synthetic method: preparation #1, McKenzie, 1971; $Ca(MnO_4)_2$ and $NaMnO_4$ were used in place of $KMnO_4$ for synthesis of Ca and Na birnessites.
27. Synthesis method: as for preparation #8 (Buser et al., Table 4) but moles HCl = 0.125; from Buser et al., 1954.
28. Synthetic method: manganese(III) manganate (IV) was prepared according to Giovanoli et al., 1970b, and was dried 10 hours at room temperature under approximately 10^{-5} torr.
29. Synthetic method: Na manganese(II,III) manganate(IV) was prepared according to Giovanoli et al., 1970a, but was not dried. The solid from 0°C oxidation was washed by filtration and kept under deionized water.
30. Frondel et al., 1960b.
31. Frondel, 1953.
32. Richmond, 1969.
33. Bardossy and Brindley, 1978.
34. Synthetic method: buserite was prepared by the method of Giovanoli (1970a) for Na manganese(II,III) manganate(IV). The oxidation product was washed with deionized water and stored as an aqueous suspension. Co and Mn analogs were prepared by the method of McKenzie, 1971.

the variation in the position of band 4. Manganese oxidation state (Table 1) is not correlated to the position of band 3.

In light of this unexplained variation in pyrolusite IR spectra, the unindexed X-ray lines, and the proven orthorhombic modification, detailed structural work on pyrolusite single crystals is warranted.

The positions and relative intensities of bands 1 and 2 uniquely and clearly distinguish pyrolusite from the other manganese oxides.

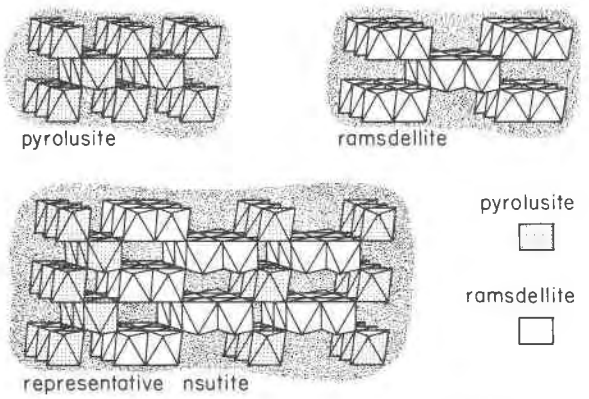

Fig. 1. Manganese oxide chain structures, looking approximately down *c* (modified from Clark, 1972, p. 228, 237).

Ramsdellite

Ramsdellite has a chain structure similar to that of pyrolusite. In ramsdellite the chains are doubled by the sharing of edges between two adjacent chains; these double chains are linked by shared vertices (Byström, 1949).

Ramsdellite has been thought to be the only other stoichiometric manganese dioxide besides pyrolusite. We have found that it invariably contains a single crystallographically-ordered water. The IR spectrum of ramsdellite is shown in Figure 4. Although we were able to obtain only one pure ramsdellite, spectra of three others were identical to Figure 4 in band number and position and with only minor variation in band intensity when absorption due to the impurities was subtracted. Bands 8, 9, and 10 are present in the spectra of all ramsdellites listed in Table 1 and are also present in pyrolusite #3, which contains ramsdellite impurity. Band 8 is due to an H_2O bending vibration. The intensity relationship of the bands indicate that the major hydrous species is H_2O; the sharpness of band 10 and the structure on band 8 indicates that the water is in a well-defined crystallographic site. The ramsdellite structure was determined for a sample containing 1.3 percent water (Byström, 1949), which is characteristic of other ramsdellite samples (Fleischer *et al.,* 1962). This water was assumed to be an impurity. The presence of a crystallographically well-ordered water in all our ramsdellite samples suggests that it may be an integral part of the structure. The intensities of the water bands are approximately the same as those for the hydrous manganese oxide romanechite (Fig. 10). The analyses in Fleischer *et al.* indicate a stoichiometry $MnO_2 \cdot 0.06H_2O$.

The overall character of the ramsdellite IR spectrum clearly distinguishes it from all other manganese oxides except the hollandite group and some synthetic nsutites. The presence of band 7 and the position of band 2 distinguish ramsdellite from the hollandite group. The presence of band 7 distinguishes it from nsutite.

Nsutite

Nsutite is a structural intergrowth of pyrolusite and ramsdellite in which layers of single and double chains alternate in random fashion (de Wolff, 1959; Laudy and de Wolff, 1963). One of the many possible structural variations is shown in Figure 1. Natural and synthetic nsutites exhibit a range of X-ray diffraction patterns which have been interpreted to be the result of variation in the concentration of pyrolusite microdomains. The changes in X-ray line sharpness, number, and position for the nsutite patterns in Figure 2 are in agreement with that expected in going from a low (#18) to a high (#17) concentration of pyrolusite microdomains (de Wolff, 1959; Laudy and de Wolff, 1963). Heat-treatment of nsutite produces a series of materials continuing this transition in X-ray powder pattern to that of a disordered pyrolusite (Gattow and Glemser, 1961a; Brenet *et al.,* 1958). These are thought to be a continuation of the structural series postulated for unheated samples (Laudy and de Wolff, 1963).

Our work supports the conclusion of Laudy and de Wolff that progressive heat-treatment of nsutite produces increasing concentrations of randomly distributed pyrolusite microdomains, but it suggests that variations in unheated samples are predominantly the result of differences in crystalline order. We have progressively heated two nsutites and in each case

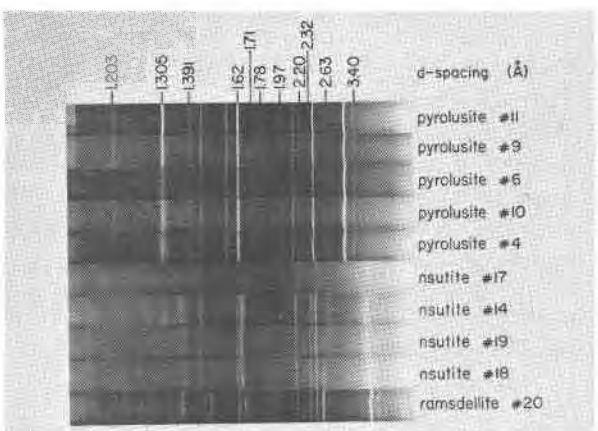

Fig. 2. X-ray powder diffraction patterns of the chain-structure manganese oxides, showing an increasing degree of orthorhombic distortion for pyrolusite.

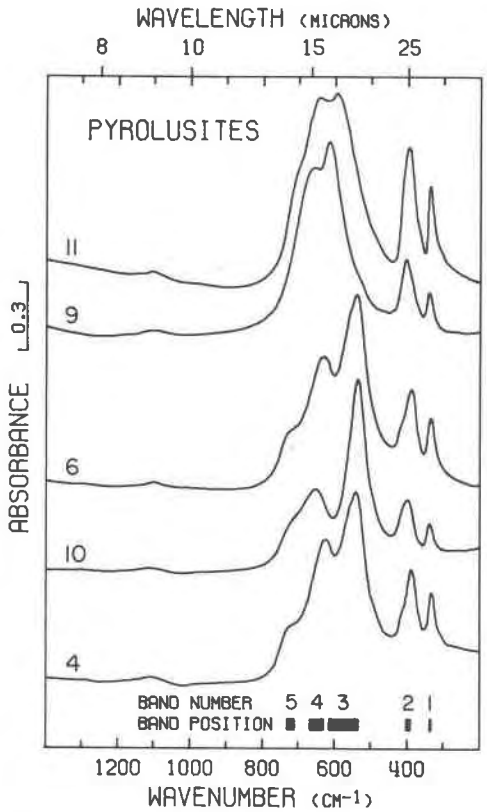

Fig. 3. IR spectra of pyrolusites. Presentation intensities: #11, 161%; #9, 112%; #6, 143%; #10, 120%; #4, 127%.

obtained a series of X-ray patterns similar to that of Brenet *et al.* Both exhibit variations in band position and intensity (Fig. 5 and 6) which cannot be reproduced by addition of various proportions of pyrolusite and nsutite spectra. They are therefore not physical mixtures of pyrolusite and nsutite, and Figures 5 and 6 indicate the effect on the IR spectrum of variation in the concentration of pyrolusite microdomains. The spectra presented in Figure 7 span the range of variation for unheated synthetic and natural nsutites. The arrangement is according to the presumed concentration of pyrolusite microdomains (increasing upward in the figure), based on the X-ray diffraction data in Figure 2. The difference in the spectra do not follow the trends for increasing concentration of pyrolusite microdomains established by Figures 5 and 6. Instead the variation is primarily one of band sharpness and relative intensity. In general, spectra of highly-ordered materials are characterized by sharp, well-defined absorption bands. As disorder increases, the bands become broader and less clearly resolved, but their wavenumber positions remain unchanged. Much of the variation in Figure 7 therefore reflects differences in the crystalline order of the samples. The decrease in sharpness and number of X-ray lines, which has commonly been interpreted as indicating a high concentration of pyrolusite microdomains, appears to be primarily indicative of disorder. We have no explanation for the variation in relative intensity of the absorption bands. The band intensity relationship for each nsutite is maintained through the heat-induced transformation to pyrolusite and is therefore unrelated to the concentration of pyrolusite microdomains. It appears to be related to the variation in the position of pyrolusite band 3, although it should be noted that pyrolusite band 3 has developed from different nsutite bands in Figures 5 and 6.

All nsutites have a broad absorption in the 3600 cm^{-1} to 3100 cm^{-1} region. This is generally of low intensity but becomes more intense with decrease in crystalline order. It is attributable primarily to water in the more disordered cases, but may be either water or hydroxyl in those samples with a higher degree of order.

Nsutite #14 in Figure 7 is characteristic of the natural samples we have studied. Natural processes at

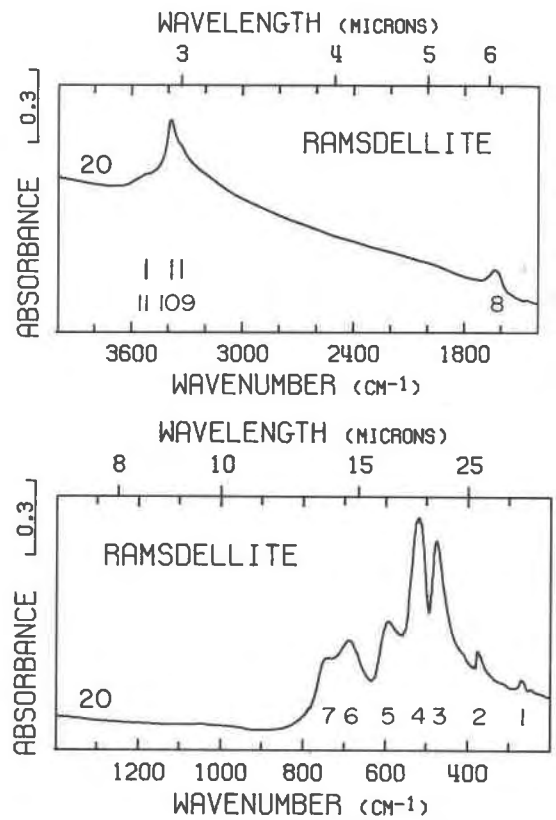

Fig. 4. IR spectrum of ramsdellite. Presentation intensity: 137%.

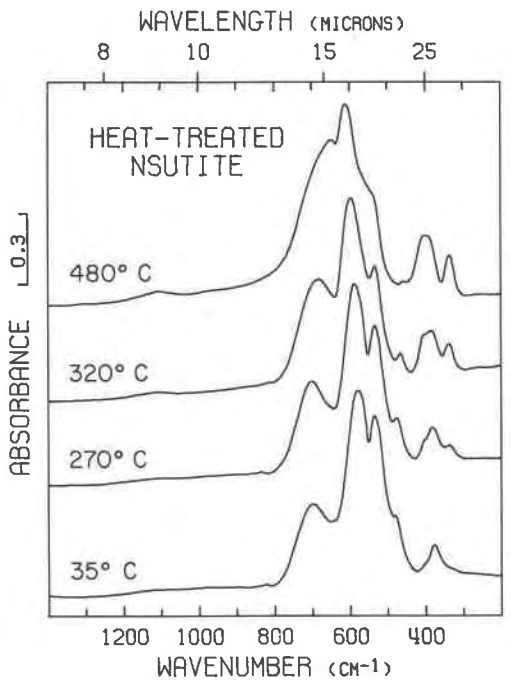

Fig. 5. The effect of progressive heat-treatment on the IR spectrum of nsutite #16. Presentation intensities: 480°C, 137%; 320°C, 120%; 270°C, 106%; 35°C, 105%.

these localities apparently produce nsutites of similar crystalline order and concentration of pyrolusite microdomains.

The positions of bands 1 and 5 (Fig. 7) distinguish natural nsutites from the hollandite group, whose spectra are similar. Synthetic nsutites which have spectra close to that of ramsdellite can be distinguished from it by band 5, which is a single band in nsutite and split in ramsdellite, and by the absence of ramsdellite bands 8 and 9.

The channel structures: the hollandite group and romanechite (psilomelane)

The hollandite group

The structure of the hollandite-group minerals (Figure 8) consists of MnO_6 octahedra which share edges to form double chains as in ramsdellite (Byström and Byström, 1950, 1951). These double chains are linked by shared vertices forming channels; Ba, K, Pb, or Na are present in the channels and coordinated to the oxygens of the double chains. The identity of the channel cations determines the mineral species.

IR spectroscopy in the 1400 cm^{-1}–200 cm^{-1} region does not distinguish among the various minerals in the hollandite group; the spectrum in Figure 9 is representative of them all. The spectral features involve the vibrations of the octahedral framework and do not include a significant contribution from the large cations in the channel. Far IR spectra for synthetic hollandite and cryptomelanes differ. Hollandite absorbs at 97 cm^{-1} and cryptomelane absorbs at 136 cm^{-1}. These absorptions might be associated with the channel constituents. Hollandite-group minerals may have either tetragonal or monoclinic symmetry (Byström and Byström, 1950). We have shown by Weissenberg single-crystal X-ray diffraction that hollandite #30 has monoclinic symmetry and cryptomelane #27 has tetragonal symmetry. No differences between the IR spectra of these samples are apparent.

Most hollandite-group samples exhibit an extremely broad, low-intensity absorption covering approximately the 3500 cm^{-1} to 2500 cm^{-1} region and a rather broad, low-intensity H_2O bending band near 1600 cm^{-1}. There must be some water in most samples; however, the broadness and weakness of the bands suggest that little is present and that it does not occupy well-defined crystallographic sites.

The spectra of our samples do not show a continuous variation between hollandite and romanechite

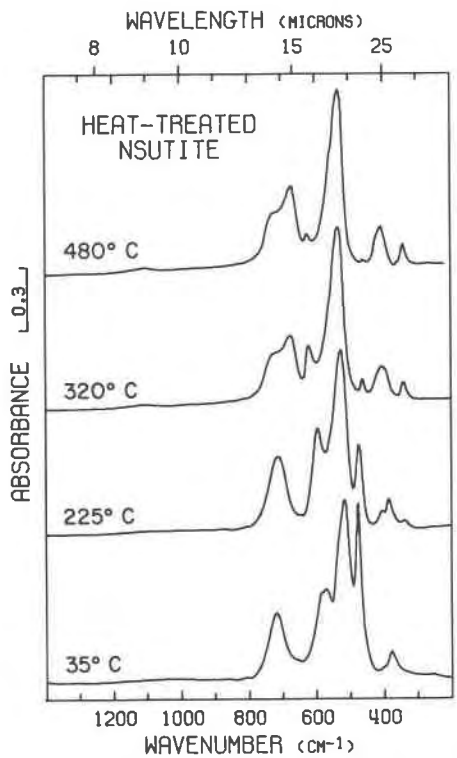

Fig. 6. The effect of progressive heat-treatment on the IR spectrum of nsutite #18. Presentation intensities: 480°C, 62%; 320°C, 47%; 225°C, 66%; 35°C, 80%.

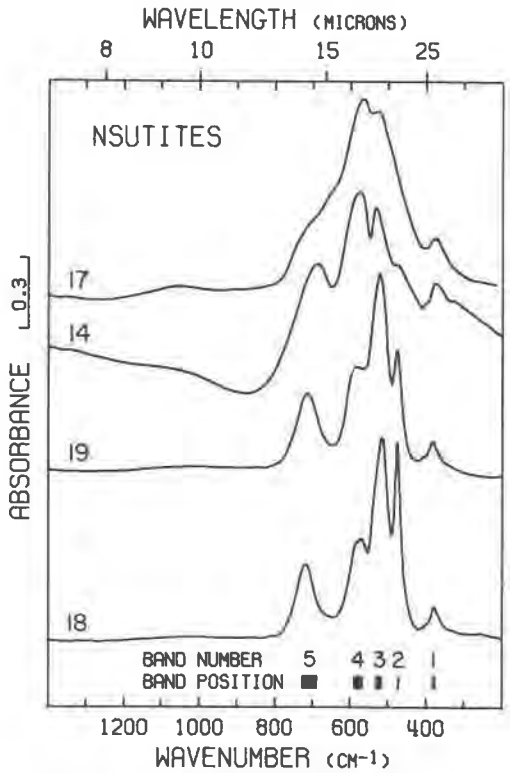

Fig. 7. IR spectra of nsutites. Presentation intensities: #17, 145%; #14, 314%; #19, 78%; #18, 80%.

which the electron microscopy studies of Turner and Buseck (1979) indicate may exist. Hollandite-group spectra are similar to those of ramsdellite, nsutite, and romanechite. Except for romanechite, these are all based structurally on the octahedral double-chain unit, but in hollandite these basic units are linked together to produce a different overall structure. In the 1400 cm^{-1} to 200 cm^{-1} region this difference is sometimes manifest in the IR spectrum only below 400 cm^{-1}, where the position of band 1 at 310 cm^{-1} is diagnostic of minerals of the hollandite group; however, the relative intensities of bands 2, 3, and 4 generally serve as an additional distinction from ramsdellite and natural nsutites. Hollandite-group minerals can be distinguished from romanechite by the additional romanechite bands (Fig. 10), particularly those in the 4000 cm^{-1} to 1400 cm^{-1} region, and by the band near 600 cm^{-1}, which is prominent in hollandite-group spectra (band 4) and generally only a weak shoulder in romanechite spectra (band 7).

Romanechite (psilomelane)

There remain some questions concerning the structure of romanechite. Wadsley (1953) determined the structure shown in Figure 8. It is similar to the hollandite structure except that the channels are broadened due to the presence of triple chains. Both water and barium are thought to be present in the channels. The structure is monoclinic. The chemical formula which is used in this paper (Table 1) is supported by the work of Fleischer (1960). Mukherjee (1959, 1965), however, indicates an orthorhombic structure and a chemical formula with hydrogen present as hydroxyl. He suggests that his differences from Wadsley are due primarily to the samples examined rather than the analyses, and that Wadsley was working on an alteration product of true romanechite.

Our work clearly resolves the uncertainty regarding the nature of the hydrous components of romanechite. Bands 9, 10, and 11 in the IR spectrum (Fig. 10) indicate a single, crystallographically-ordered type of water. They resemble, in intensity and position, the water found in channels of such minerals as beryl and cordierite (Goldman *et al.*, 1977, 1978). The broad absorption on the low wavenumber side of band 10 may be due to a second, less-ordered wa-

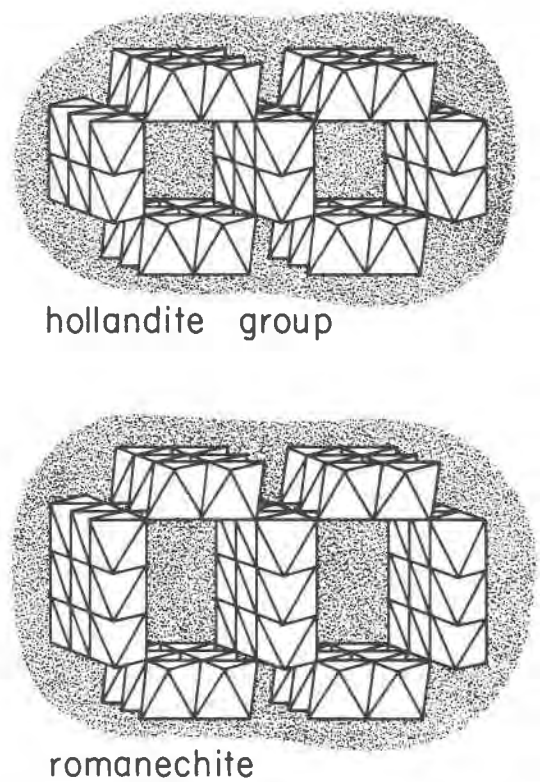

Fig. 8. Manganese oxide channel structures, looking approximately down the channels (modified from Clark, 1972, p. 237). In the hollandite group, Ba, K, Pb, or Na are present in the channels: romanechite channels contain Ba and H_2O.

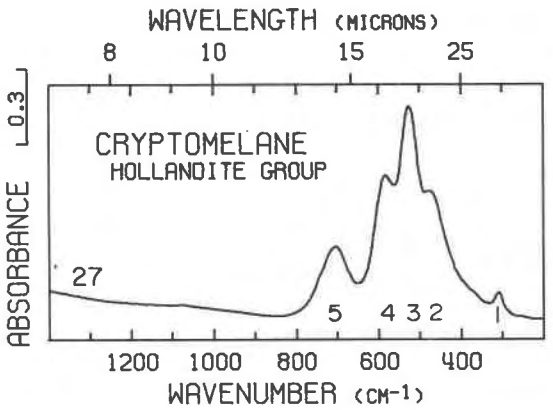

Fig. 9. IR spectrum of cryptomelane, which is representative of the hollandite group. Presentation intensity: 133%.

ter, but is more likely an artifact due to the Christiansen effect (Prost, 1973), a result of refractive index mismatch between TlBr and the sample. The IR spectrum shows no evidence for hydroxide ions. The intensity of the water bands varies from sample to sample, indicating a variable water content in accord with the chemical data of Fleischer (1960) for other romanechites. These results are in accord with the formula of Wadsley, in which the hydrous component is water, and inconsistent with that of Mukherjee, in which hydrogen is present as hydroxide ion. These water IR features are characteristic of all the romanechites listed in Table 1 with the exception of #35, which has negligible absorption due to hydrous components. It thus appears that water rather than hydroxide ion is characteristic of romanechite. Our evidence suggests that our samples are analogous to that of Mukherjee. Both samples which were X-rayed gave powder patterns whose line positions and relative intensities are in good agreement with Mukherjee's sample.

Figure 10 is representative of the spectra of all the romanechites of Table 1. There is negligible variation in band position and, with the exception of band 4, in relative band intensity. Figure 10 shows the maximum relative intensity observed for band 4. In some instances it is present only as a prominent shoulder.

The same major bands are present in romanechite as in the nsutites, ramsdellite, and the hollandite group, but the relative intensities differ. For romanechite, band 7 is invariably a weak shoulder, band 6 a major band. In addition, bands 3 and 4 are peculiar to romanechite. Bands 1 and 2 are diagnostic of romanechite, although the latter is so weak as to be missed in poorly crystalline samples. The positions and sharpness of bands 9, 10, and 11 are diagnostic of romanechite and are clearly recognizable in most samples.

The layer structures: chalcophanite, aurorite, and lithiophorite

Chalcophanite and aurorite

The chalcophanite structure (Wadsley, 1955) is based on layers of edge-shared MnO_6 octahedra (Fig. 11). One out of seven octahedral sites in the MnO_6 layer is vacant. These alternate with layers of zinc and layers of water in the stacking sequence: Mn–O–Zn–H_2O–Zn–O–Mn. All waters are thought to be structurally equivalent, with weak hydrogen-bonding between water molecules. Our work supports Wadsley's inferences regarding the nature of the hydrous component. Bands 11, 12, and 13 are characteristic of water in a single, crystallographically-ordered site. The band position indicates approximately the same

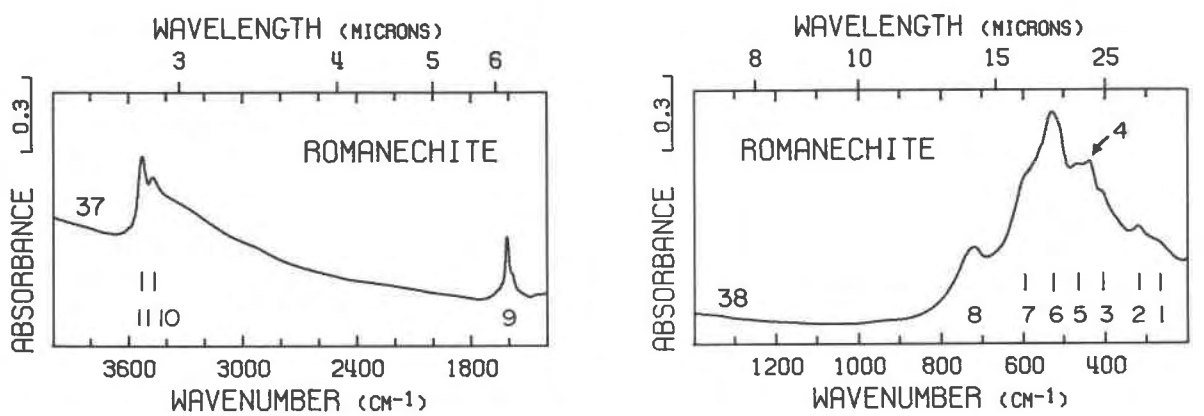

Fig. 10. IR spectrum of romanechite (psilomelane). Different samples were chosen for each spectral region to best illustrate the IR features. Presentation intensity: 251%.

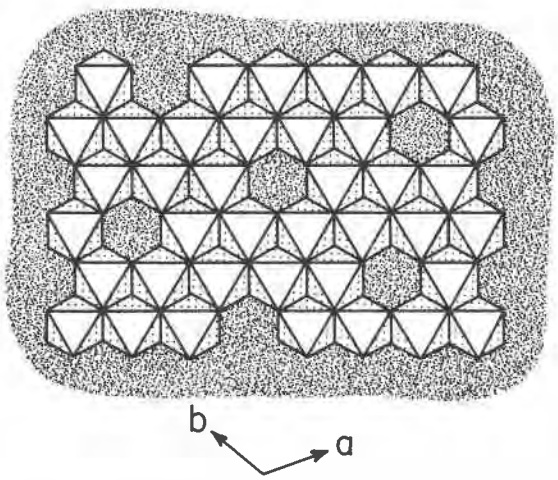

Fig. 11. Chalcophanite MnO_6 layer structure, the *ab* plane.

degree of hydrogen-bonding as in liquid water. The IR spectrum of the other chalcophanite in Table 1 matches Figure 12 exactly except for minor variation in relative band intensity.

X-ray powder diffraction patterns indicate that aurorite has the chalcophanite structure (Radtke *et al.*, 1967). We have confirmed this. The absorption bands in the IR spectrum are identical in number and position to those of chalcophanite although there are some differences in relative intensity.

The position and sharpness of bands 12 and 13 and the sequence of four bands in the 550 cm^{-1} to 400 cm^{-1} region distinguish chalcophanite and aurorite from all other manganese oxides.

Lithiophorite

The structure of lithiophorite (Wadsley, 1952) consists of layers of edge-shared octahedra similar to those of chalcophanite but with all octahedral sites filled. These layers alternate with layers of $(Al,Li)(OH)_6$ octahedra. There is no ordering of the Al and Li in these octahedral sites. Wadsley suggested that hydrogen bonding exists between layers and that the hydroxide ions are aligned perpendicular to the layers.

Our work confirms Wadsley's suggestions regarding the nature of the hydrous component. The single, sharp, absorption band near 3400 cm^{-1} together with the nearly complete absence of the water bending mode near 1600 cm^{-1} in the spectrum of #42 (Fig. 13) indicates that a single type of hydroxide ion predominates. In addition, in the well-crystallized sample there are two weak shoulders on the low-energy side of band 11 which are resolved at liquid nitrogen temperature. Single-crystal, polarized IR reflectance work shows that all three bands are polarized perpendicular to the basal cleavage. The hydroxide ions are thus aligned in this direction. The lower-intensity bands may correspond to hydroxide in local environments created by statistically less probable populations of Al and Li atoms in nearby octahedral sites.

Lithiophorite can be distinguished from all other manganese oxides by the intensity and position of band 11 and by the presence of band 9. The positions of all the bands in the intensity relationship of Figure 13 are also diagnostic of lithiophorite. Both well-crystallized (#42) and poorly-crystallized (#43) samples are shown.

Incompletely characterized structures: birnessite, todorokite, buserite, woodruffite, and rancieite

Considerable confusion exists with respect to the structural natures and relationships of the materials

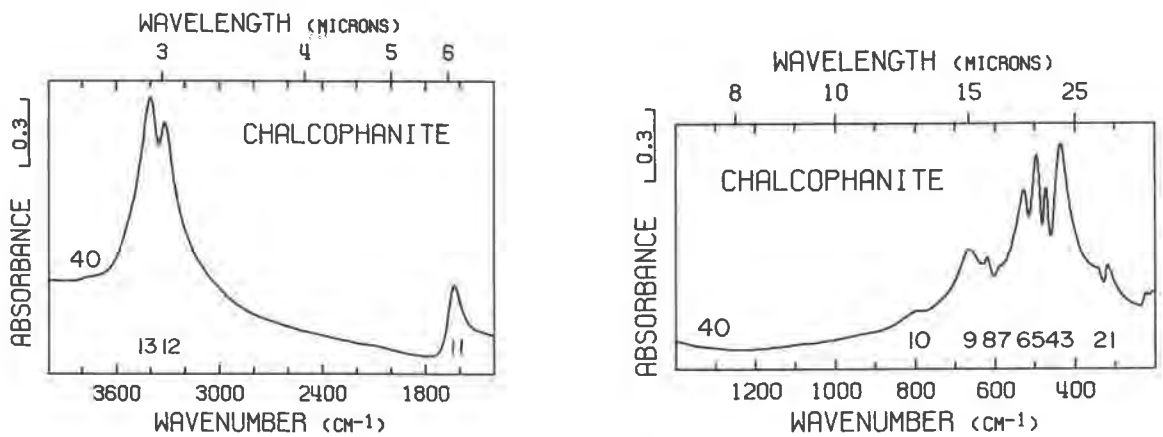

Fig. 12. IR spectrum of chalcophanite. Presentation intensity: 161%.

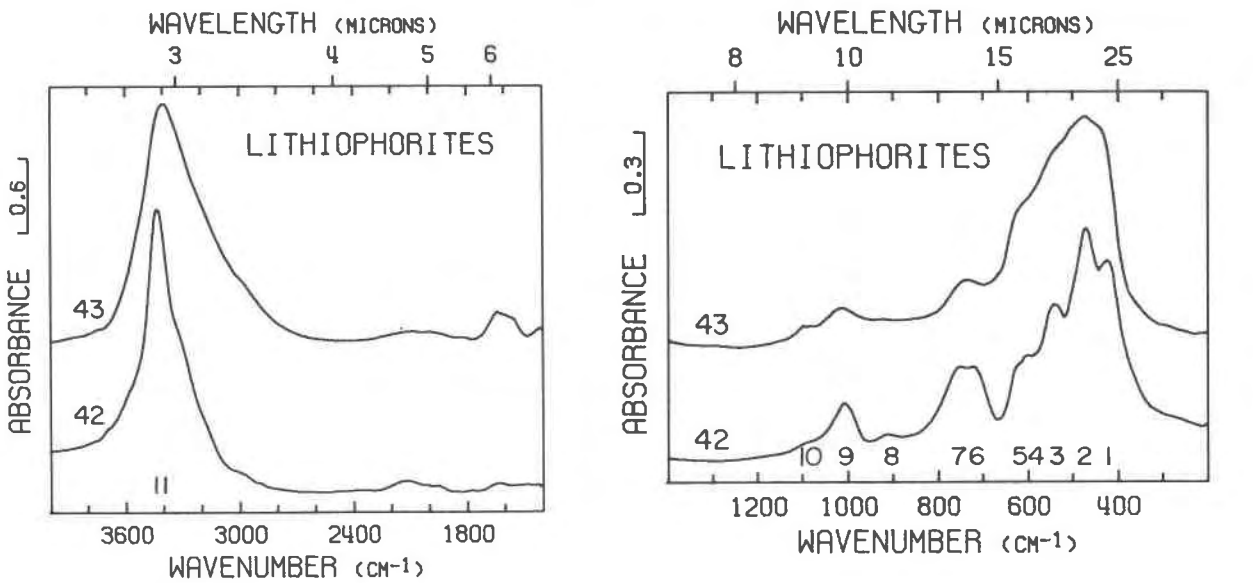

Fig. 13. IR spectra of lithiophorites. Presentation intensities: #43, 172%; #42, 173%.

considered in this section. This is a direct result of the poor response of X-ray diffraction to their minute particle sizes, poor crystalline order, and structural variations within a mineral group. The natural samples we have examined indicate that birnessite, todorokite, and rancieite, when well-crystallized, are structurally distinct from one another. With increasing disorder, however, the structural distinctions among them become more subtle or vanish altogether. We feel that the structural differences among these three merit their consideration as distinct mineral phases and have consequently organized this section with a subsection for each. The synthetic phase buserite may be related to birnessite but is included in a separate subsection to facilitate discussion.

Birnessite

Giovanoli (1969) has suggested that birnessite occurs in an infinity of structural varieties all based on the same crystal lattice but differing in crystallite size, lattice order, manganese oxidation state, and cation substitution. Our work supports this view. IR spectra of both natural and synthetic birnessites show variation in band position and, to a larger extent, relative band intensity (Fig. 14). Such variations do not occur for those manganese oxides with a single, well-defined structure, but are characteristic of the structurally-variable nsutite. Nevertheless, the general similarity of the spectra strongly suggests that most birnessite samples are characterized by the same basic structures. The one exception is #54. Most of its bands are shifted by 20–40 cm^{-1} from those of other samples, and it differs from all others in the absence of band 7 and the splitting of band 4.[4] The sharpness of its bands indicates that it has a higher degree of order than the other samples. Structural changes relating to this ordering could be responsible for the band shifts. We have classed sample #54 as a structural variant of the birnessite group but we do not feel that the data are compelling evidence for this.

The basic structure of the birnessite group has been inferred from the postulated structures of sodium manganese(II,III) manganate(IV) (our birnessite #54) and manganese(III) manganate(IV) (our birnessite #51) (Giovanoli *et al.*, 1970a,b). Although there is some question of the validity of the former as a synthetic birnessite, the latter is clearly a representative of the group as a whole. The proposed structure is similar to that of chalcophanite. MnO_6 octahedral layers have a vacancy in one out of every six octahedral sites. These are separated by layers of lower-valent cations and by layers of water and hydroxide ions. Our work has several implications which support this structure. The positions of the major bands in the 1400 cm^{-1} to 200 cm^{-1} region suggest that birnessites have a layer structure, as discussed in a later section. The fact that the identity of

[4] The higher wavenumber component of band 4, sample #54, may actually correlate to band 5.

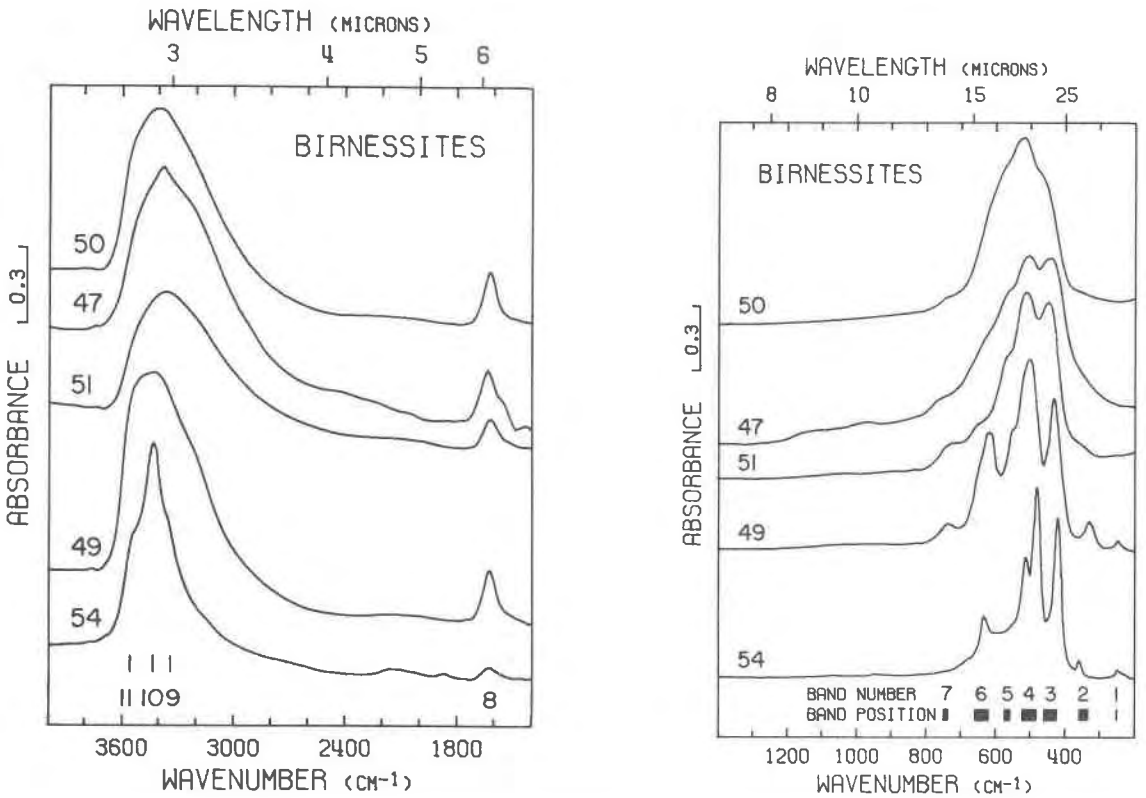

Fig. 14. IR spectra of birnessites. Presentation intensities: #50, 106%; #47, 247%; #51, 99%; #49, 104%; #54, 53%.

the large cations does not influence these bands suggests that the cations are weakly bound to the MnO_6 octahedral layers. We interpret the 4000 cm^{-1} to 1400 cm^{-1} pattern as follows: a hydroxide ion in a specific crystallographic site produces band 10, and a less-ordered water produces the remaining features.

The spectra in Figure 14 are arranged in order of increasing band sharpness, which reflects crystalline order. In general, X-ray powder patterns do not follow this trend. This suggests the presence in some samples of a disordered component to which X-ray diffraction is insensitive.

Natural birnessite is distinguished from most of the manganese oxides by the presence of bands 3 and 4 as two broad features. It can be distinguished from poorly-ordered chalcophanite and generally from todorokite by the features in the 4000 cm^{-1} to 1400 cm^{-1} region. It can be distinguished from rancieite by the position of band 7 near 750 cm^{-1}, by the absence of rancieite band 4 near 700 cm^{-1}, and generally by the relative intensity and positions of the two major bands. Synthetic birnessite can be distinguished by these criteria and, for well-ordered material, by the general character of the spectrum. Some samples may be difficult to distinguish from highly disordered todorokite.

Birnessite vs. vernadite (δ-MnO_2)

δ-MnO_2, also called vernadite, is a hydrous, slightly crystalline material which usually shows only two X-ray diffraction lines at 1.4 and 2.4A. Because, in part, these are two of the strongest birnessite lines, Giovanoli (1969) considered δ-MnO_2 and birnessite to be two members of a single group. Giovanoli *et al.* (1973) suggest that members of the birnessite group show a continuum of variation in crystalline order. On the basis of electron diffraction, Chukhrov *et al.* (1978a, b) concluded that birnessite and vernadite have different *c* parameters and are appropriately considered different mineral species.

Chukhrov *et al.* presented IR spectra of a birnessite and several vernadites and concluded that differences in the IR pattern of the two materials supported their conclusion that they are different mineral species. Their birnessite had prominent bands at 510 and 470 cm^{-1} whereas the best vernadite pattern had the corresponding bands at 500 and 435 cm^{-1}. We note that both of the bands in both ma-

terials fall within the range of variation in the spectra of our birnessite samples. In particular, sample #47, our best-quality, natural birnessite would probably be considered a vernadite by the IR criteria of Chukhrov *et al.* The spectrum of δ–MnO_2 is not included in our compilation because all the synthetic and natural "δ–MnO_2" samples which we examined had a 7A line in their X-ray powder camera data and were therefore classified as birnessites.

Buserite

We have found buserite to be structurally analogous to its partially dehydrated product, sodium manganese(II,III) manganate(IV). The shift from 10A to 7A in the X-ray patterns is the result of water loss alone, rather than a structural rearrangement of the manganese octahedral framework. Buserite is thus analogous to some clay minerals which can undergo a collapse in basal spacing due to loss of water.

Sodium buserite was prepared by the procedure of Giovanoli *et al.* (1970). Its X-ray powder pattern in aqueous suspension matched that reported by Wadsley (1950a). Its IR spectrum (Fig. 15) was obtained in two ways. First, a TlBr pellet was prepared in the usual way except that the sample was added to powdered TlBr as a thick water slurry and the pellet was not pressed under vacuum. The resulting pellet was surrounded by water as it came from the press, and a high concentration of liquid water is shown to be present within the pellet by the intensity of the H_2O stretch and bending bands near 3400 cm^{-1} and 1600 cm^{-1} (not shown) and the broad vibrational bands in the 600 cm^{-1} to 850 cm^{-1} region (Fig. 15). We believe that the buserite in the TlBr pellet has not been dehydrated, but we are unable to show this by X-ray diffraction due to its low concentration in the TlBr. Therefore we obtained the spectrum of buserite in a petroleum jelly mull. Buserite in water suspension was dropped onto filter paper. When the excess water was removed by the capillary action of the paper, the resulting paste was mixed with petroleum jelly, sandwiched between two TlBr plates and run *vs.* a petroleum jelly–TlBr blank. Subsequent X-ray diffraction of the mull showed that no dehydration had occurred. The 10A line remained without a trace of a 7A line, although there was some alteration of the relative intensities of the other lines. The spectrum of sodium buserite from this mull technique (Fig. 15) has considerable absorption from liquid water in the 800 cm^{-1} to 600 cm^{-1} region. Comparison of the buserite spectrum with that of its dehydration product, sodium manganese(II,III) manganate(IV) (Fig. 14, #54) indicates that no significant structural rearrangement of the manganese octahedral framework has occurred during dehydration. The close similarity of the spectra of cation-exchanged buserites to that of sodium buserite supports those conclusions. The materials do not dehydrate so readily as sodium buserite and can be air-dried without losing the 10A spacing. We have found that the spectra of both manganese and cobalt buserites differ from that of sodium buserite only in the sharpness of the bands, which reflects crystalline order. Giovanoli *et al.* (1975) have concluded that the 10A manganese oxide phases are hydrates of the 7A phases. Insofar as buserite and sodium manganese(II,III) manganate(IV) are concerned, our work supports this.

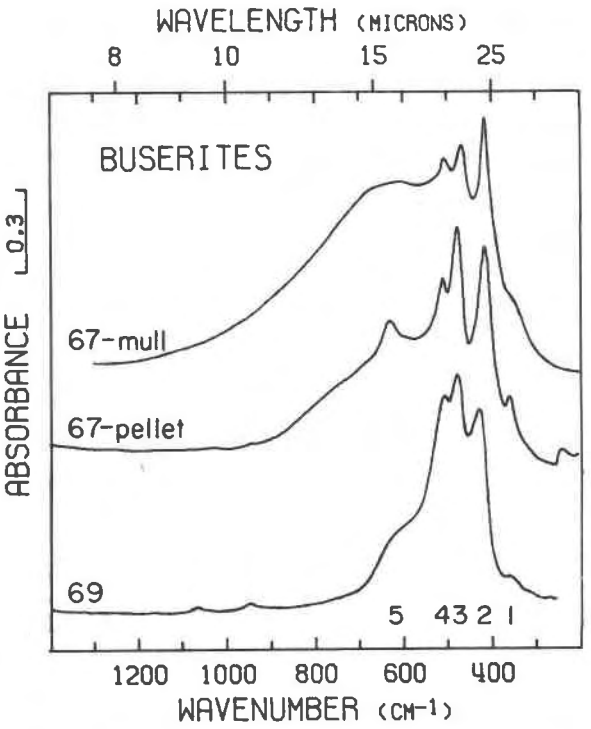

Fig. 15. IR spectra of buserite. The top spectrum was obtained by the petroleum jelly mull technique described in the text. The middle spectrum was obtained by the wet TlBr pellet technique described in the text, presentation intensity: 72%. The bottom spectrum was obtained normally, presentation intensity: 97%.

Well-crystallized buserite is distinguished from all other manganese oxides except sodium manganese(II,III) manganate(IV) by the positions and relative intensities of its IR features in the 1400 cm^{-1} to 200 cm^{-1} region. When highly disordered it may be difficult to tell from some birnessites and from highly-disordered todorokite.

Todorokite and woodruffite

The validity of todorokite as a single mineral phase has been questioned (Giovanoli *et al.*, 1971; Giovanoli and Bürki, 1975). On the basis of electron microscopy and electron diffraction, they concluded that it is a mixture of buserite and the products of its dehydration (birnessite) and reduction (manganite). None of the todorokite samples we have examined can be such a mixture; our work strongly suggests that todorokite is a valid mineral species. The variation in todorokite IR spectra (Fig. 16) is predominantly one of crystalline order. There is little variation in band position, and the spectrum of even the most disordered material retains indications of all but the most minor bands of the well-crystallized material. The large variation in relative band intensities expected for a mixture of phases is absent in the 1400 cm^{-1} to 200 cm^{-1} region. The variation in intensity of bands 16 and 17 is due to an increasing ratio of absorbed water to crystallographic water with decreasing crystalline order.

The spectrum characteristic of todorokite cannot be produced by the addition of the spectra of buserite, birnessite, and manganite. Our todorokites do not show evidence for manganite, although as little as 5% could be recognized from the sharp metal–hydroxide bands near 1100 cm^{-1} and the hydroxyl bands near 2700 cm^{-1} and 2100 cm^{-1} (Fig. 4A). No combination of the bands of other manganese oxides can duplicate the water–hydroxide ion bands of the todorokite spectrum. Such a characteristic IR spectrum with complex features not attributable to other known phases is strong evidence for a specific, characteristic structure.

Comparison of the buserite and todorokite spectra show that buserite is not a todorokite analog. The water and hydroxide bands of the two materials have no similarity, and there is no correspondence between most of the bands in the 1400 cm^{-1} to 200 cm^{-1} region unless they are shifted up to 40 cm^{-1}. Natural todorokites do not show such large band shifts. Synthetic todorokites prepared by cation exchange of buserite (McKenzie, 1971) are incorrectly named.

The structure of todorokite is not known. Crystal morphology and cleavage suggest that todorokite has a channel structure similar to hollandite or romanechite (Burns and Burns, 1975, 1977a, b). Our work suggests that it has a layer structure. This will be considered in detail in a later section. Our work also

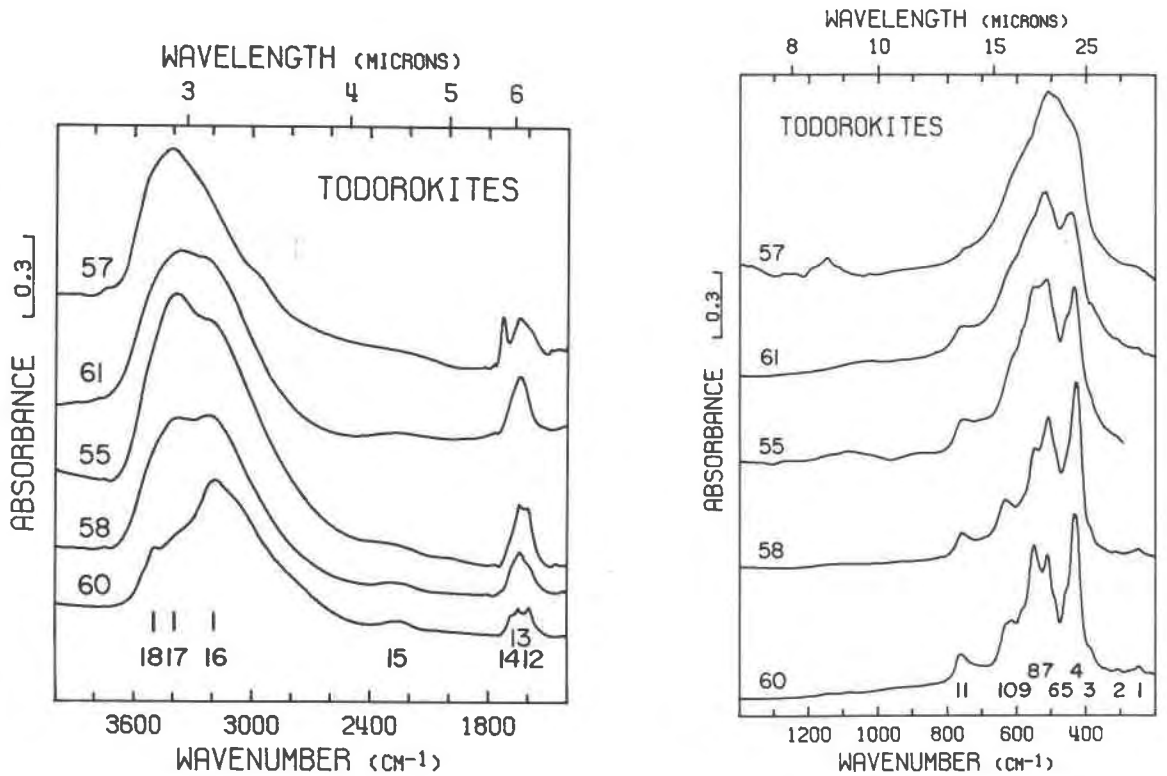

Fig. 16. IR spectra of todorokites. Presentation intensities: #57, 91%; #61, 192%; #55, 198%; #58, 86%; #60, 106%.

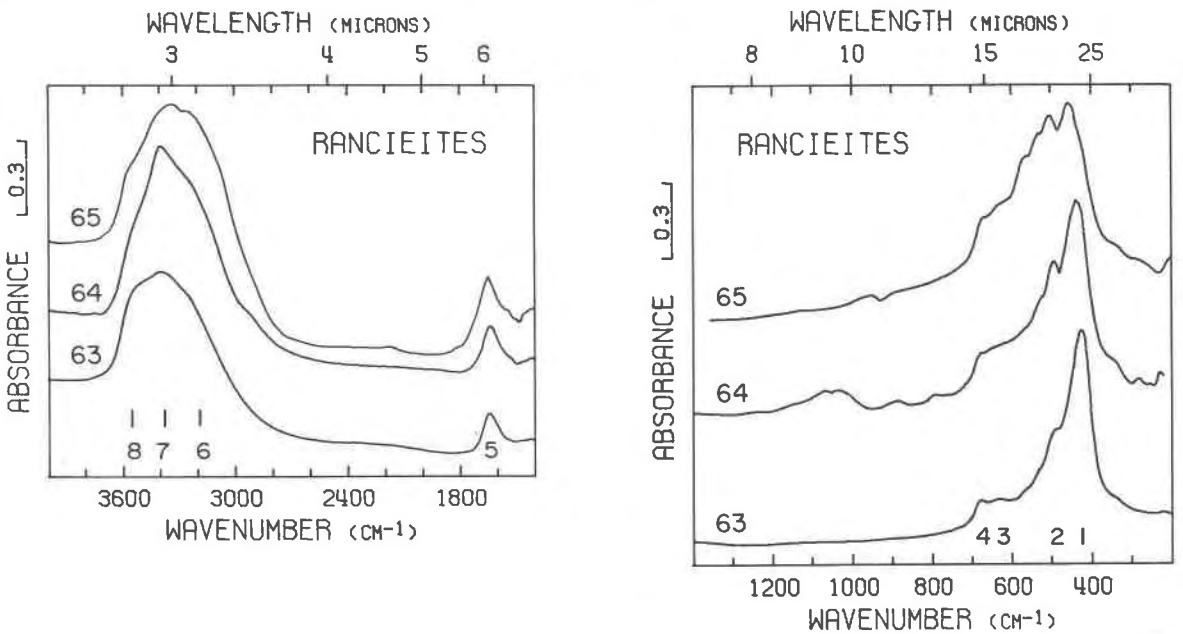

Fig. 17. IR spectra of rancieites. Presentation intensities: #65, 478%; #64, 115%; #63, 62%. The absorption of braunite impurity has been removed from the spectrum of #65 (text footnote 5).

places constraints on the identity and structural nature of the hydrous components. The three sharp features near 1600 cm^{-1} seen for the best-ordered material indicate multiple water environments in well-defined crystallographic sites. Band 17 reflects a low degree of hydrogen bonding. The position of the major band near 3200 cm^{-1} indicates that the dominant hydrogen-containing species is strongly hydrogen-bonded in the well-ordered samples. For todorokites of lower crystalline order the position of the major band near 3400 cm^{-1} suggests that the dominant species is disordered water with a lower degree of hydrogen bonding. Assessment of band 15 is uncertain.

The spectrum of woodruffite shows it to be a structural analog of todorokite, as has been assumed from the similarity of their X-ray powder patterns (Frondel, 1953).

Todorokite and woodruffite can generally be identified by the presence of band 16. Band 11 and the three intense bands in the 600 cm^{-1} to 400 cm^{-1} region (bands 4, 7, and 8) are diagnostic of all but the highly disordered samples. Highly disordered samples may be difficult to distinguish from some birnessite samples.

Rancieite

The structure of rancieite is not known. On the basis of X-ray powder diffraction data, Bardossy and Brindley (1978) have suggested that it differs from the birnessite layer structure only in the identity of the interlayer cation, and they raise the possibility that rancieite and birnessite might better be considered minerals of the same group. Giovanoli (personal communication, 1978) has examined samples from the type locality (Rancié Mine, Ariège, France) and considers them to be within the variation observed for birnessite and the 10A manganese oxides.

Our work supports the conclusion that rancieite has a layered structure closely related to that of birnessite, but it indicates that the two structures do have significant differences in the arrangement of their manganese octahedral frameworks, and they should be considered as separate minerals. In the 4000 cm^{-1} to 1400 cm^{-1} region spectra of rancieite and birnessite are indistinguishable. This indicates that the structural nature of the hydrous components is the same for the two minerals. In the 1400 cm^{-1} to 200 cm^{-1} region, the spectra of some rancieite samples (Fig. 17, #65) are nearly indistinguishable from

[5] We used a difference technique to remove braunite absorption. An intense braunite IR band occurs at 950 cm^{-1}, where there is not absorption by rancieite. The intensity of this band in the rancieite spectrum is a measure of the braunite contamination. This band was nulled in Fig. 17, #65, by subtracting the spectrum of pure braunite (Fig. 1A) at 7.2 percent of its measured intensity, thereby removing braunite absorption in the entire 1400 cm^{-1} to 200 cm^{-1} range.

those of some birnessites, but other rancieite spectra (Fig. 17, #63) differ significantly. Those rancieite samples with the most distinctive IR patterns are those for which the characteristic rancieite softness and color (Palache *et al.*, 1944, p. 572; Richmond *et al.*, 1969) are most apparent. The structural implication of the rancieite spectra will be considered more fully in the next section.

Most rancieite samples can be distinguished from other manganese oxides by the high relative intensity of the band 1. Some samples can easily be confused with disordered todorokite or birnessite; however, rancieite band 4 at 680 cm^{-1} distinguishes rancieite from these other two, which absorb at 760 cm^{-1} and 750 cm^{-1} respectively.

General relations of infrared spectra to structure

The IR spectra of the manganese oxides, except for lithiophorite, are dependent only on the MnO_6 octahedral framework. If bands in the spectra are the result of vibrations in which the large cations participate significantly, then changes in the mass of these cations should be reflected in the spectra. However, substitution in the hollandite group and the birnessites leaves the spectra in the mid-infrared region unchanged. Neither could the effect of cation substitution be seen for chalcophanite and aurorite and for todorokite and woodruffite, although the extent of the change is less since it involves incomplete substitution involving elements of relatively similar mass. Therefore we conclude that the large cations are not involved in the bands in this region of spectra. Only for lithiophorite, where light atoms other than manganese form a major part of the crystal structure, are bands in the 1400 cm^{-1} to 200 cm^{-1} region clearly attributable to other cations. Lithiophorite bands near 1000 cm^{-1} and 900 cm^{-1} are probably due to (Al,Li)–OH. The reason for this insensitivity may be that the bands are relatively weak and therefore absorb at lower energies. Hollandite and cryptomelane spectra differ in the 200 cm^{-1} to 30 cm^{-1} region, and the difference may be due to the identity of the channel cations. An alternative explanation is that the large cations are at too low a concentration in the structures to give observable bands. Although mid-infrared spectroscopy is insensitive to the channel and interlayer cations, it is diagnostic of the structural group.

The spectra provide some indication of the polymerization by edge-sharing of the MnO_6 octahedra in manganese oxides. In Fig. 18 the positions of the major bands of those minerals with known structure are plotted *vs.* their average MnO_6 octahedral polymerization. A trend is observed showing a general decrease in band energy with increasing octahedral polymerization. The point for manganosite (Fig. 5A) is included as well.[6] This trend can be used in conjunction with a direct comparison of IR patterns to infer unknown structures. The positions of the low-energy bands of birnessite support its proposed layer structure (Giovanoli *et al.*, 1970 a, b), which places it at 4.8 shared edges per octahedron.

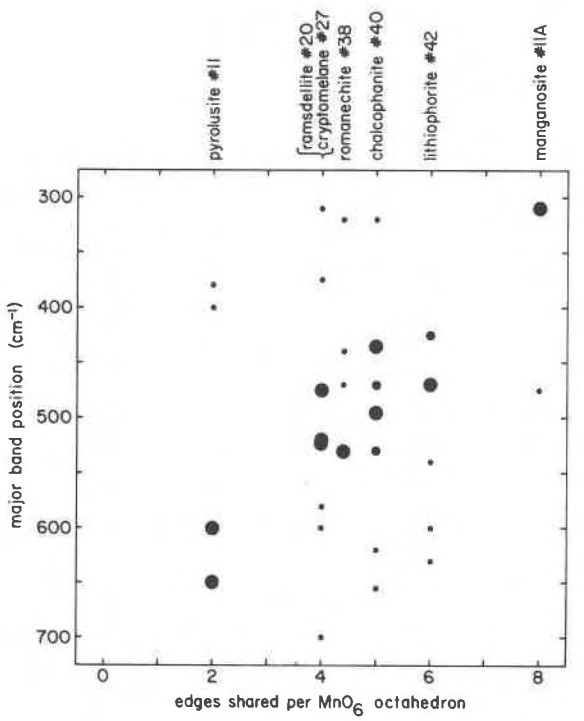

Fig. 18. Correlation of octahedral polymerization with major IR band positions. Dot size approximately proportional to band intensity. Intense absorption band positions define a trend which relates to octahedral edge-sharing.

The spectra of todorokite suggest that its structure is based on MnO_6 octahedral layers. The positions and intensities of the major bands of todorokite samples with the highest crystalline order suggest a polymerization near 5 shared edges per octahedron. This is consistent with a highly polymerized chain or

[6] Manganosite, MnO, has the NaCl structure. Being a Mn^{2+} mineral it is not strictly applicable to a trend involving predominantly Mn^{4+} minerals; however, the similarity in the positions of the low-energy bands of ramsdellite and groutite (Fig. 7, Fig. 2A), which have analogous structures (Byström, 1949; Dent Glasser and Ingram, 1968) and differ in oxidation state, suggests that structure rather than oxidation state is the dominant factor in determining band position.

channel structure and with a layer structure containing some vacancies. In order to attain a polymerization of 5 shared edges per octahedron in a chain or channel structure it is necessary to build them from units whose average polymerization is 5. This corresponds to quadruple chains. No chain or channel manganese oxides composed of such large units are known to exist, although isolated quadruple chains have been observed in hollandite in electron microscope images (Turner and Buseck, 1979). It appears that for highly polymerized structures a layer structure is preferred. Direct comparison of todorokite spectra to those of other manganese oxides supports this. All known layer structures have a strong band in the 400 cm^{-1} to 450 cm^{-1} region, which is analogous to todorokite band 4 at 430 cm^{-1}. Strong absorption in this region does not occur for the chain and channel structures. These suggestions contrast with previous work which suggests that todorokite has a channel structure (Burns and Burns, 1977a). This was based on the needle-like morphology of todorokite and the presence of two perfect cleavage planes seen under the electron microscope. Todorokite occurs in other morphologies as well. Todorokite #58 has a platy morphology reminiscent of birnessite. Weissenberg single-crystal X-ray diffraction indicates that the sample is ordered in the same plane as the plates but disordered in planes perpendicular to them. This suggests that it consists of a random superposition of single-crystal todorokite plates and eliminates the possibility that it is a mass of needles that appear morphologically as a plate.

The spectra of rancieite suggest a polymerization near 6 shared edges per octahedron, which corresponds to a filled octahedral layer.

Spectra of samples of birnessite, todorokite, and rancieite may be similar in the 1400 cm^{-1} to 200 cm^{-1} region. For birnessite and todorokite this similarity is related to crystalline disorder. For the most disordered birnessite and todorokite, the IR spectra are similar (*e.g.*, #50 and #57). Interestingly, because the X-ray order does not necessarily follow the IR order, sample #57 is readily identified as todorokite from the X-ray pattern, whereas sample #50 has a diffuse X-ray pattern, barely recognizable as birnessite. As the order increases, the spectra of the two minerals become more distinct from one another. This suggests that birnessite and todorokite are built of fundamentally similar units and that it is the ordering of these units which makes the minerals distinct from one another. We believe that this is the case for rancieite as well, but our data could also be interpreted as evidence for a structural continuum from well-crystallized birnessite (Fig. 14, #54) to well-crystallized rancieite (Fig. 17, #63). In this case the smooth change in relative intensity and position of rancieite band 1 (Fig. 17) would reflect the degree of birnessite "character."

The lower valent manganese oxides

We have included as Appendix A spectra of well-characterized samples of the following lower valent manganese oxides: braunite, groutite, hausmannite, manganite, manganosite, partridgeite and quenselite.[3] In some cases these are necessary for the interpretation of the earlier sections of the paper. Others are included so that this paper may serve as a compilation of the spectra of all manganese oxides commonly encountered in nature. They illustrate the ability of infrared spectroscopy to produce patterns diagnostic for each mineral phase for the whole range of naturally occurring manganese oxides. It extends the usefulness of this paper as a data base for further structural work on the manganese oxide.

Conclusions

Infrared spectroscopy has proven to be a useful tool for the mineralogical identification of the tetravalent manganese oxides. Different oxides can be distinguished by absorption patterns due to vibrations of the MnO_6 octahedral framwork in the 1400 cm^{-1} to 200 cm^{-1} region. The 4000 cm^{-1} to 1400 cm^{-1} region is often diagnostic due to absorption associated with the hydrous components of the oxides.

Because of its sensitivity to short range order, infrared spectroscopy gives more reliable information than X-ray diffraction when applied to disordered and finely particulate samples. With X-ray diffraction a small amount of well-crystallized material in a disordered or finely particulate matrix can give the impression that the whole sample is well-crystallized. The lack of correspondence between the degree of order indicated by these two techniques for our birnessite samples as a manifestation of this effect. X-ray diffraction data alone could lead to an error in mineralogical identification of the disordered material if a well-crystallized minor component of different mineralogy is present. For minerals which have only a few characteristic X-ray diffraction lines, such as birnessite, todorokite, and rancieite, infrared spectroscopy has shown that X-ray diffraction alone may be an insufficient test for the validity of synthetic analogs.

IR spectroscopy can also contribute to the determi-

nation of the structures and structural relationships among the tetravalent manganese oxides. We have been able to suggest features of the unknown oxide structures based on their IR spectra and the relation of these spectra to those of manganese oxides with known structure. We have applied IR spectroscopy to the role of water and hydroxide ion, whose presence and structural orientations can only be inferred from X-ray and chemical data.

Now that IR spectra of well-characterized manganese oxide samples are available to serve as standards, this technique should find wider application for mineralogical identification of manganese oxides in the terrestrial and aquatic environments.

Acknowledgments

We thank the following for providing samples for this study: J. S. White, Jr., Smithsonian Institution; C. G. Cunningham, U. S. Geological Survey; A. R. Kampf, Los Angeles County Museum of Natural History; R. G. Burns and V. M. Burns, Massachusetts Institute of Technology; A. J. Bauman, Jet Propulsion Laboratory; G. W. Brindley, Pennsylvania State University; A. S. Corey, Pasadena City College; V. Morgan, Boron, California; L. Dalbec, Ridgecrest, California; and R. Currier, Arcadia, California. A small portion of the funding for this work was provided by the L. S. B. Leakey Foundation and the John A. McCarthy Foundation. Helpful critical reviews were provided by R. G. Burns and R. Giovanoli, Berne.

References

Agiorgitis, G. (1969) Uber differential-thermoanalytische und infrarotspektroscopische Untersuchungen von Mangan-Mineralien. *Tschermaks Mineral. Petrogr. Mitt., 13,* 273–283.

Bardossy, G. and G. W. Brindley (1978) Rancieite associated with a karstic bauxite deposit. *Am. Mineral., 63,* 763–767.

Brenet, J. P., J. P. Gabano and M. Seigneurin (1958). Transformations thermiques d'oxydes de manganese. In *Papers Presented To The Section On Inorganic Chemistry (16th International Congress Of Pure And Applied Chemistry, Paris, 1957),* p. 69–80. Butterworth Scientific Publications, London.

Brown, F. H., A. Pabst and D. L. Sawyer (1971) Birnessite on colemanite at Boron, California. *Am. Mineral., 56,* 1057–1064.

Burns, R. G. and V. M. Burns (1975) Structural relationships between the manganese(IV) oxides. In A. Kozawa and R. J. Brodd, Eds., *Manganese Dioxide Symposium,* Vol. 1, p. 306–327. The Electrochemical Society, Cleveland.

——— and ——— (1977a) Mineralogy. In G. P. Glasby, Ed., *Marine Manganese Deposits,* Chapt. 7. Elsevier, Amsterdam.

——— and ——— (1977b) The mineralogy and crystal chemistry of deep-sea manganese nodules, a polymetallic resource of the twenty-first century. *Phil. Trans. R. Soc. Lond., A286,* 283–301.

Buser, W., P. Graf and W. Feitknecht (1954) Beitrag zur Kenntnis der Mangan(II)-manganite und des δ-MnO_2, *Helv. Chim. Acta, 37,* 2322–2333.

Byström, A. M. (1949) The crystal structure of ramsdellite, an orthorhombic modification of MnO_2. *Acta Chim. Scand., 3,* 163–173.

Byström, A. and A. M. Byström (1950) The crystal structure of hollandite, the related manganese oxide minerals, and α-MnO_2. *Acta Crystallogr., 3,* 146–154.

——— and ——— (1951) The positions of the barium atoms in hollandite. *Acta Crystallogr., 4,* 469.

Champness, P. E. (1971) The transformation manganite → pyrolusite. *Mineral. Mag., 38,* 245–248.

Chukrov, F. V., A. I. Gorshkov, E. S. Rudnitskaya, V. V. Berezovskaya and A. V. Sivtsov (1978a) On vernadite. (in Russian) *Izvest. Akad. Nauk. SSSR, Ser. Geol.,* 5–19.

———, E. S. Rudnitskaya and A. V. Sivtsov (1978b) The characteristics of birnessite. (in Russian) *Izvest. Akad. Nauk. SSSR, Ser. Geol.,* 67–76.

Clark, G. M. (1972) *The Structures of Non-molecular Solids: A Coordinated Polyhedron Approach.* Applied Science Publishers, London.

Cole, W. F., A. D. Wadsley and A. Walkley (1947) An X-ray diffraction study of manganese dioxide. *Trans. Electrochem. Soc., 92,* 133–158.

de Wolff, P. M. (1959) Interpretation of some γ-MnO_2 diffraction patterns. *Acta Crystallogr., 12,* 341–345.

Dent Glasser, L. S. and L. Ingram (1968) Refinement of the crystal structure of groutite, α-MnOOH. *Acta Crystallogr., 24,* 1233–1236.

Farmer, V. C. (Ed.) (1974) *The Infrared Spectra of Minerals.* Mineral Society of London, London.

Finkelman, R. B., H. T. Evans, Jr. and J. J. Matzdo (1974) Manganese minerals in geodes from Chihuahua, Mexico. *Mineral. Mag., 39,* 549–558.

Fleischer, M. (1960) Studies of the manganese oxide minerals. III. Psilomelane. *Am. Mineral., 45,* 176–187.

——— and G. T. Faust (1963) Studies on manganese oxide minerals VII. Lithiophorite. *Schweiz. Mineral. Petrogr. Mitt., 43,* 197–216.

———, W. E. Richmond and H. T. Evans, Jr. (1962) Studies of the manganese oxides V. Ramsdellite, MnO_2, an orthorhombic dimorph of pyrolusite. *Am. Mineral., 47,* 47–57.

Frondel, C. (1953) New manganese oxides hydrohausmannite and woodruffite. *Am. Mineral., 38,* 761–769.

———, U. B. Marvin and J. Ito (1960a) New data on birnessite and hollandite. *Am. Mineral., 45,* 871–875.

———, ——— and ——— (1960b) New occurrences of todorokite. *Am. Mineral., 45,* 1167–1173.

Gattow, G. and O. Glemser (1961a) Darstellung und Eigenshaften von Braunsteinen. II (Die γ- und η-Gruppe der Braunsteine). *Z. anorg. allg. Chem., 309,* 20–36.

——— and ——— (1961b) Darstellung und Eigenshaften von Braunsteinen. III (Die ϵ, β, und α-Gruppe der Braunsteine, uber Ramsdellite und uber Umwandlungen der Braunsteine). *Z. anorg. allg. Chem., 309,* 121–232.

Giovanoli, R. (1969) A simplified scheme for the polymorphism in the manganese dioxides. *Chimia, 23,* 470–472.

——— and P. Burki (1975) Comparison of X-ray evidence of marine manganese nodules and nonmarine manganese ore deposits. *Chimia, 29,* 266–269.

———, ——— and P. Scheiss (1973) Investigation of manganese nodules. Report #33a, *Universitat Bern.* [English tradition of introduction. Quoted in Burns and Burns (1977a)].

———, ———, M. Gioffredi and W. Stumm (1975) Layer structured manganese oxide hydroxides. IV: The buserite group, structure stabilization by transition elements. *Chimia, 29,* 517–520.

———, W. Feitknecht and F. Fischer (1971) Reduktion von Mangan(III)-manganat(IV) mit Zimtalkohol. *Helv. Chim. Acta, 54,* 1112–1124.

———, R. Maurer and W. Feitknecht (1967) Zur Struktur des γ-MnO_2. *Helv. Chem. Acta., 50,* 1072–1080.

———, E. Stahli and W. Feitknecht (1970a) Uber Oxidhydroxide des vierwertigen Mangansmit Schichtengitter 1. Mitteilung: Natrium—mangan(II,III) manganat(IV). *Helv. Chim. Acta, 53,* 209–220.

———, ——— and ——— (1970b) Uber Oxidhydroxide des vierwertigen Mangans mit Schiechtengitter 2. Mitteilung: Mangan(III)-manganat(IV). *Helv. Chim. Acta, 53,* 453–464.

Glemser, O., G. Gattow and H. Meisiek (1961) Darstellung und Eigenschaften von Braunsteinen. I (Die δ-Gruppe der Braunsteine). *Z. anorg. allg. Chem., 309,* 1–19.

Goldman, D. S., G. R. Rossman and W. A. Dollase (1977) Channel constituents in cordierite. *Am. Mineral., 62,* 1144–1157.

———, ——— and K. M. Parkin (1978) Channel constituents in beryl. *Phys. Chem. Mineral., 3,* 225–235.

Gruner, J. W. (1947) Groutite, $HMnO_2$, a new mineral of the diaspore–goethite group. *Am. Mineral., 32,* 654–659.

Kolta, G. A., F. M. A. Kerim and A. A. A. Azim (1971) Infrared absorption spectra of some manganese dioxide modifications and their thermal products. *Z. anorg. allg. Chem., 384,* 260–266.

Laudy, J. H. A. and P. M. de Wolff (1963) X-ray investigation of the δ–β transformation of MnO_2. *Appl. Sci. Res. Sect., B10,* 157–168.

McKenzie, R. M. (1971) The synthesis of birnessite, cryptomelane, and some other oxides and hydroxides of manganese. *Mineral. Mag., 38,* 294–502.

Mitchell, R. S. and A. S. Corey (1973) Braunite and surassite from Los Angeles County, California. *Mineral. Rec., 4,* 290–293.

Moenke, H. (1962) *Mineral Spectren.* Akademie-Verlag, Berlin.

Moore, T. E., M. Ellis and P. W. Selwood (1950) Solid oxides and hydroxides of manganese. *J. Am. Chem. Soc., 72,* 856–872.

Mukherjee, B. (1959) X-ray study of psilomelane and cryptomelane. *Mineral. Mag., 32,* 166–171.

——— (1967) Crystallography of psilomelane, $A_3X_6Mn_8O_{16}$. *Mineral. Mag., 35,* 645–655.

Palache, C., H. Berman and C. Frondel (1944) *Dana's System of Mineralogy,* Vol. I. Wiley, New York.

Potter, R. M. and G. R. Rossman (1979a) The manganese and iron oxide mineralogy of desert varnish. *Chem. Geol., 25,* 79–94.

——— and ——— (1979b) A magnesium analogue of chalcophanite in manganese-rich concretions from Baja California. *Am. Mineral., 64,* 1227–1229.

——— and ——— (1979c) Mineralogy of manganese dendrites and coatings. *Am. Mineral., 64,* 1219–1226.

Prost, R. (1973) The influence of the Christiansen effect on I. R. spectra of powders. *Clays Clay. Mineral., 21,* 363–368.

Radtke, A. S., C. M. Taylor and D. F. Hewett (1967) Aurorite, argentian todorokite and hydrous silver-bearing lead manganese oxide. *Econ. Geol., 62,* 186–206.

Richmond, W. E., M. Fleischer and M. E. Mrose (1969) Studies on manganese oxide minerals. IX rancieite. *Bull. Soc. fr. Mineral. Cristallogr., 92,* 191–195.

Segeler, C. G. (1959) Notes on a second occurrence of groutite. *Am. Mineral., 44,* 877–878.

Turner, S. and P. R. Buseck (1979) Manganese oxide tunnel structures and their intergrowths. *Science, 203,* 456–458.

Valarelli, J. V., M. Perrier and G. Vicentini (1968) Infrared spectra of some manganese minerals. *An. Acad. brasil Ciênc., 40,* 289–296.

van der Marel, H. W. and H. Beutelspacher (1976) *Atlas of Infrared Spectra of Clay Minerals and Their Admixtures.* Elsevier, Amsterdam.

Vaux, G. and H. Bennet (1937) X-ray studies on pyrolusite (including polianite) and psilomelane. *Mineral. Mag., 24,* 521–526.

Wadsley, A. D. (1950a) A hydrous manganese oxide with exchange properties. *J. Am. Chem. Soc., 72,* 1782–1784.

——— (1950b) Synthesis of some hydrated manganese minerals. *Am. Mineral., 35,* 485–499.

——— (1952) The structure of lithiophorite, $(Al,Li)MnO_2(OH)_2$. *Acta Crystallogr., 5,* 676–680.

——— (1953) The crystal structure of psilomelane, $(Ba,H_2O)_2Mn_5O_{10}$. *Acta Crystallogr., 6,* 433–438.

——— (1955) The crystal structure of chalcophanite, $ZnMn_3O_7 \cdot 3H_2O$. *Acta Crystallogr., 8,* 165–172.

Zwicker, W. K., W. O. J. Groeneveld Meijer and H. W. Jaffe (1962) Nsutite—a widespread manganese oxide mineral. *Am. Mineral., 47,* 246–266.

Manuscript received, February 12, 1979;
accepted for publication, June 25, 1979.